An-Najah University Journal for Research - B (Humanities)

Volume 37 | Issue 10 Article 6

2023

Analysis of Normalized Difference Vegetation Index change of the West Bank, Palestine, Using Multitemporal Satellite Remote Sensing Data

ahmed Ghodieh
1Department Of Geography & Geomatics, Faculty of Economics and Social Sciences, An-Najah National University, Nablus, Palestine, ahmed@najah.edu

An - Najah Univ. J. Res. (Humanities). Vol. 37(10), 2023

Analysis of Normalized Difference Vegetation Index change of the West Bank, Palestine, Using Multitemporal Satellite Remote Sensing Data

التحليل القياسي لمؤشر الفروق الطبيعية للغطاء النباتي في الضفة الغربية، فلسطين، باستخدام بيانات الاستشعار عن بعد للأقمار الصناعية في فترات مختلفة

Ahmed Ghodieh[1,*]

أحمد غضية[1]

[1]Department Of Geography & Geomatics, Faculty of Economics and Social Sciences, An-Najah National University, Nablus, Palestine

[1]قسم الجغرافيا والجيوماتكس، كلية الاقتصاد والعلوم الاجتماعية، جامعة النجاح الوطنية، نابلس، فلسطين

*Corresponding author: ahmed@najah.edu

Received: (18/8/2022), Accepted: (21/11/2022)
DOI: 10.35552/0247.37.10.2089

Abstract

The West Bank is characterized by the diversity of its climate despite its small area. It includes four climatic regions:- a humid, semi-humid, arid, and semi-arid climate. This in turn affected the geographical distribution of vegetation cover seasonally and over the years. This study investigated changes in the West Bank, Palestine vegetation cover using multitemporal Landsat data. Four images were selected for this purpose – two corresponding to 2001 and the other two corresponding to 2021. Seasonal change of the Normalized Difference Vegetation Index (NDVI) was investigated for the acquired images. ArcGIS 10.8 software was used for image processing and analysis. Results showed that the negative change of the NDVI of autumn for both dates is much higher than the positive change. About 98.89 percent of the West Bank area scored a negative change in 2001, while about 80.79 percent of the West Bank

scored a negative change in 2021. The negative change in autumn is due to the dryness of summer season, which in turn led to the drying of the green grasses and herbs that grow among the trees and on the eastern slopes of the highlands. Concerning the NDVI change between 2001 and 2021, results showed a considerable positive change in the NDVI. Around 90.91% of the surface area of the West Bank (5132.304 km²) has positive change, while only 9.09% (513.405 km²) which mainly represents urban centers has negative change. The main reason that the NDVI in 2021 was higher than the NDVI in 2001 outside the urban centers is that the amount of rain in that year was greater, especially in the northern areas. Thematic maps of NDVI for the two dates were produced, and changes in vegetation cover were extracted from the four maps. Based on the results of the study, it is recommended that decision-makers in the Ministry of Agriculture and Environmental organizations develop plans to increase permanent green spaces, especially in arid and semi-arid areas of the West Bank.

Keywords: NDVI, West Bank, Vegetation, Agriculture, Satellite Data.

ملخص

تتميز الضفة الغربية بالتنوع المناخي على الرغم من صغر مساحتها، فهي تشتمل على اربعة اقاليم مناخية: الاقليم الرطب، الاقليم شبه الرطب، الاقليم الجاف، والاقليم شبه الجاف. هذا التنوع المناخي اثر على التوزيع الجغرافي للغطاء النباتي فصليا وعلى مدى سنوات طويلة. تناولت هذه الدراسة التغيرات في كثافة الغطاء النباتي للضفة الغربية، فلسطين، باستخدام بيانات القمر الصناعي لاندسات بأوقات مختلفة. تم اختيار أربع مرئيات فضائية لهذا الغرض - اثنتان في عام 2001 والصورتان الأخريان في عام 2021. تم فحص التغيير الموسمي لمؤشر الفروق الطبيعية للغطاء النباتي (NDVI) من تلك المرئيات. كما تم استخدام برنامج ArcGIS 10.8 لمعالجة الصور وتحليلها. أظهرت النتائج أن التغير السلبي لمؤشر NDVI للخريف لكلا التاريخين أعلى بكثير من التغير الإيجابي. سجل حوالي 98.89 في المائة من مساحة الضفة الغربية تغيراً سلبياً في عام 2001، بينما سجل حوالي 80.79 في المائة من الضفة الغربية تغيراً سلبياً في عام 2021. ان التغير السلبي لمؤشر النبات يعود الى جفاف فصل الصيف والذي بدوره ادى الى جفاف النباتات الخضراء والحشائش التي تنمو بين الاشجار وعلى المنحدرات الشرقية للمرتفعات. وفيما يتعلق بتغير مؤشر NDVI بين عامي 2001 و2021، أظهرت النتائج تغيراً إيجابياً ملحوظاً في مؤشر NDVIحوالي 90.91٪ من مساحة الضفة الغربية (5132.304 كيلومتر مربع)، بينما 9.09٪ فقط (513.405 كيلومتر مربع) والتي تمثل بشكل رئيسي المراكز العمرانية، لديها تغير سلبي.

السبب الرئيسي في كون مؤشر النبات في عام 2021 كان اعلى من عام 2001 خارج حدود المناطق العمرانية هو ان كمية الامطار كانت اعلى في ذلك العام، وخاصة في المناطق الشمالية. تم إنتاج الخرائط الموضوعية NDVI للتاريخين، وتم استخلاص التغييرات في الغطاء النباتي من الخرائط الأربع. بناء على النتائج، فان الدراسة توصي اصحاب القرار في وزارة الزراعة والمؤسسات البيئية بتطوير خطط لزيادة المساحات الخضراء في الضفة الغربية، خاصة في المناطق الجافة وشبه الجافة.

الكلمات المفتاحية: NDVI، الضفة الغربية، الغطاء النباتي، الزراعة، بيانات الأقمار الصناعية.

Introduction

Vegetation cover affects the local and regional environment. The economy of local communities and millions of people in developing countries depends on forests, plants, and pastures (Mokarram & Sathya Moorthy, 2015). Vegetation cover also effectively protects people against natural hazards such as rockfalls, landslides, and floods (Jin *et al*., 2009). Remote sensing is regarded as one of the most powerful tools for studying the spatial distribution of vegetation. Data from remote sensing systems such as the Advanced Very High-Resolution Radiometer (AVHRR), the Moderate Resolution Imaging Spectroradiometer (MODIS), Landsat, and SPOT are appropriate for studying the Normalized Difference Vegetation Index (NDVI) of large- and medium-sized areas (Friedl *et al*., 2002).

The NDVI is considered to be one of the important measures and indicators of green vegetation cover density and greenness (Buchhorn *et al*., 2016). It is also used to evaluate vegetation biomass and health (Chen *et al*., 2009). The NDVI has been used extensively to examine the relationship between spectral variability and the changes in vegetation growth rate. It is also used to estimate the production of green vegetation as well as to detect changes in vegetation (Singh, 2021). The NDVI is a synthetic image layer created from the existing wavebands of multispectral and hyperspectral remote sensing data (Ju & Bohrer, 2017). This new layer adds new information not found in the original individual wavebands. Low red (R) band reflectance and high near infrared (NIR) reflectance of green vegetation help perform a band rationing of these two wavebands (Huang *et al*. 2013). Therefore, the NDVI is calculated using the R and the NIR

wavebands. Mathematically, the NDVI is the ratio of the difference between the NIR waveband and the R waveband and the sum of these two wavebands, i.e., NDVI = (NIR -R)/ (NIR + R) (Yengoh *et al*., 2014). The value of the NDVI ranges between -1 and +1 (Mokarram *et al*., 2016). Brighter pixels of the NDVI layer are correlated with more biomass and have positive values, while water, shadows, and moist soil have negative digital number (DN) values. Rocks, dry soil, and senescent vegetation and crops have DN values near zero (Zhai *et al*., 2022).

A number of scholarly articles have investigated the use of multispectral remote sensing data for studying the NDVI and the land cover. Abuelaish and Olmedo (2016) used five Landsat images and GIS data to study land use change in the Gaza Strip, Palestine.

Ghodieh (2019) used multitemporal aerial photographs and satellite images to estimate urban land use change in the West Bank, Palestine. Singh and Javeed (2021) used the NDVI to assess the land cover changes in Srinagar district in Kashmir. They used multitemporal data for the years 2001 and 2017 from Landsat 7 and Landsat 8 data. Their results show an increase of urban and barren lands by around 4%, while the densely vegetated areas decreased from around 8% to 2% from 2001 to 2017.

Buchhorn *et al*. (2016) investigated the influence of bidirectional reflectance distribution function (BRDF) on the NDVI and biomass estimations of Alaska Arctic tundra. They found that studies that sampled only a narrow range of biomass and NDVI produced equations that were more difficult to correct for BRDF effects.

Ju and Bohrer (2017) used the NDVI time series from NASA's HLS dataset for classifying wetland vegetation. Their results reveal how changes in water elevation have modified the patch distribution in significant ways, leading to the local extinction of certain types of vegetation by 2019 and a continuous increase in the area cover of some other vegetation types.

Ndungu *et al*. (2019) used MODIS NDVI to monitor Kenyan rangelands through a web-based decision support tool. They found that the

tool they used requires improvement to provide decision-makers with more accurate and adequate results.

Zhu *et al*. (2021) used multitemporal MODIS NDVI imagery and a digital elevation model to explore variations in the growing season NDVI and its response to climate change. Their results show that there are significant changes with fluctuations in NDVI values from 2000 to 2017.

Yengoh *et al*. (2015) used the NDVI to assess land degradation at multiple scales. They issued a report that reviews the use of NDVI for a range of themes related to land degradation.

Huang *et al*. (2021) summarized the progress of NDVI acquisition, underlined the areas of NDVI application, and addressed the critical problems and considerations in using NDVI.

Gutman (1999) used long-term global data of land reflectance and vegetation indices derived from AVHRR. Their study illuminated the aspects of time-series analysis with the available global AVHRR data and suggested ways to improve these data for interannual variability studies.

Mokarram and Sathyamoorthy (2015) investigated the relationship between elevation, aspect, and spatial distribution of vegetation in Darab Mountain, Iran, using remote sensing data. They found that vegetation growth and vegetation indices increase with increasing elevation and aspect.

Gandhi *et al*. (2015) used an enhanced change detection method for analyzing satellite images based on the NDVI. The simulation results confirm that the NDVI is highly useful in detecting the surface features of the visible area, which are extremely beneficial for policymakers in decision-making.

Jin *et al*. (2009) used MODIS NDVI imagery to quantify the spatial distribution of vegetation. The results obtained by analyzing NDVI data for seven years clearly indicate that elevation and aspect, as a proxy for precipitation and temperature, are very important factors for the vertical distribution of vegetation.

Robinson *et al*. (2017) addressed the deficits of high-resolution NDVI data by producing a Landsat-derived, high-resolution (30 m), long-term (30+ years) NDVI dataset for the conterminous United States. They used Google Earth Engine, a planetary-scale cloud-based geospatial analysis platform, for processing the Landsat data and distributing the final dataset. Towers and Echeverría (2021) investigated the effect of the illumination angle on NDVI data composed of mixed surface values obtained over vertical-shoot-positioned vineyards (VSP). The results confirmed that factors that intervene in determining the direction of illumination on a VSP will alter the integrated NDVI value.

Alessandro and Salvatore (2021) suggested the use of unmanned aerial vehicle (UAV) for studying the NDVI and other crop attributes instead of using traditional satellite imagery. They clarified that the UAV had high spatial resolution, unlike the coarse spatial resolution of satellite imagery, and thus, results of NDVI analysis would be more accurate.

Naif *et al*. (2020) investigated the seasonal variations in the NDVI in the city of Baghdad, Iraq. They found a strong relationship between temperature and precipitation and the NDVI. They also noticed a negative correlation between temperature and the NDVI and a positive correlation between precipitation and the NDVI. In their study,

Huang *et al*. (2013) quantified the influence of spectral response functions on the R and NIR reflectance values and NDVI derived from 31 Earth observation satellite sensors. Their results show various degrees of differences of the R, NIR, and NDVI values of satellite sensors.

Ma *et al*. (2020) examined the effect of seasonal and spatial variations in solar zenith angle (SZA) on retrieving vegetation phenology from time series of the NDVI and Enhanced Vegetation Index (EVI) across a study area in southeastern Australia. They noted that NDVI sensitivity to SZA was on average nearly five times greater than EVI sensitivity.

Zhai *et al*. (2022) derived the tasseled cap transformation (TCT) coefficients for Landsat 8 surface reflectance independently and top of atmosphere (ToA) reflectance using the Gram–Schmidt orthogonalization method. The results demonstrate that the derived Landsat-8 TCT

coefficients can effectively characterize brightness, greenness, and wetness components across the CONUS and show good consistency for discrimination of land cover types and track seasonal surface variations.

Zaitounah *et al*. (2018) used remote sensing technology and GIS to detect changes in land cover and NDVI quickly and accurately in Besitang watershed, Indonesia. They observed that the land cover with the highest NDVI value range with a very dense vegetation density class is the primary dry forest.

The Research Problem and Aims

Despite its small size, the West Bank is distinguished by the diversity of its climate. It has four climatic regions: humid, semi-humid, arid, and semi-arid. This, in turn, influenced the seasonal and long-term geographical distribution of vegetation cover. The green vegetation cover of the West Bank has not been studied carefully in terms of density and spatial distribution using modern geographical technologies, such as remote sensing and geographic information systems (GIS). The first goal of this research is to investigate green vegetation cover using moderate-resolution multitemporal remote sensing data (Landsat data). The second goal is to investigate the geographical distribution of green vegetation density, and the third goal is to detect seasonal changes in green vegetation cover between 2001 and 2021.

Materials and Methodology

Study Area

The study area or the West Bank of the River Jordan lies between the latitudes 31° 20´ and 32° 38´ N and between the longitudes 34° 53´ and 35° 31´ E. Its surface area including the north-western part of the Dead Sea and East Jerusalem is 5860 km². Its length from north to south is around 130 km, and its average width from west to east is 40 km (Figure 1).

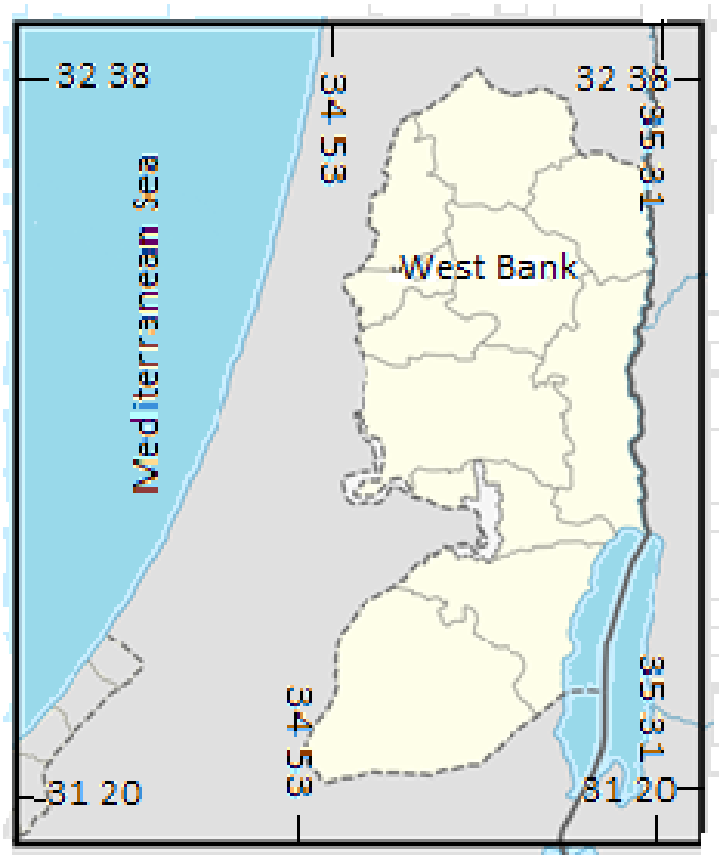

Figure (1): Location map of the study area (Ghodieh, 2019).

The study area consists of four main topographic and climatic regions: the semi-coastal region, the mountain region, the eastern slope region, and the Jordan valley region (Hamada & Ghodieh, 2021) (Figure 2). The semi-coastal and the mountain regions belong to the Mediterranean climate and receive a good amount of rainfall (500–700 mm/ year), while the eastern slope region and the Jordan valley region belong to the semi-arid climate and receive a small amount of rainfall (100–350 mm/ year). Also, annual average temperatures of the coastal and mountain regions are moderate (16°C–18°C), while those of the eastern slope and the Jordan valley regions are higher (20°C–23°C) (Arij, 2003).

These topographic and climatic characteristics of the West Bank have affected the spatial distribution of vegetation cover on the one hand, and the population distribution on the other hand. The semi-coastal and the mountain regions are characterized with denser vegetation cover than the eastern slope and the Jordan Valley regions. Vegetation cover of the semi-arid regions is limited to the alluvial plains and valleys. Agriculture in the eastern slope region and the Jordan Valley region depends on irrigation from groundwater wells, because rain-fed agriculture is not suitable in these two regions.

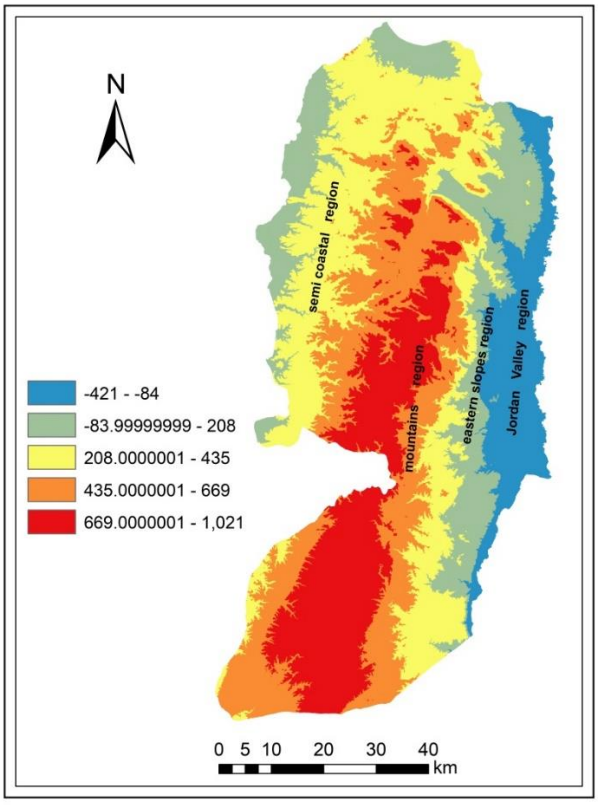

Figure (2): Topography of the West Bank (Hamada & Ghodieh, 2021).

Data

Four satellite images for the West Bank were used to accomplish this study (Table 1) (Themistocleous *et al*. 2013; Pettinari *et al*., 2016). Free Landsat-TM (Landsat 5) and Landsat- OLI (Landsat 8) images were acquired from the United States Geological Survey (USGS) website for the years 2001 and 2021. Images of the year 2001 were acquired on March 29 and October 7, representing spring and autumn, respectively, while the corresponding images of the year 2021 were acquired on April 5 and October 14. According to the Worldwide Reference System, the study area is located in path 174 and row 38. All datasets are appropriate for the study because they were cloud-free, and land cover appears clearly on all four satellite images. Also, the time span (20 years) is adequate to evaluate the NDVI change. The four satellite images were geo-referenced to the Palestine Grid 1923 coordinate system.

Methodology

The required satellite data for this study were downloaded from the USGS website (https://earthexplorer.usgs.gov). Each image covers around 185*185 km. Using ArcGIS-10.8 software and Envi 5.3 software, wavebands of each image were combined into one layer, and clipped to the boundaries of the study area (the West Bank). Also, each image coordinate system was transformed from the Universal Transverse Mercator (UTM) projection to the national Palestinian projection (Palestine Grid 1923).

Table (1): Characteristics of the satellite data used in the study (Themistocleous & Hadjimitsis, 2013; Pettinari, *et al*. 2016).

	Landsat 5	**Landsat 8**
Sensor	Thematic Mapper (TM)	Operational Land Imager (OLI) and the Thermal InfraRed Sensor (TIRS)
Swath width (km)	185	185
Number of wavebands	7	11
Bands	Blue-green, green, red, near infrared, shortwave infrared, thermal infrared, shortwave infrared	Deep blue, blue, green, red, near infrared, shortwave infrared1, shortwave infrared2, panchromatic, shortwave infrared3, thermal infrared1, thermal infrared2
Spatial resolution	Bands 1–5+7 (30 m), band 6 (120 m)	Bands 1–7+9 (30 m), band 8 (15 m), bands 10 and 11 (100 m resampled to 30 m)
Radiometric resolution	8 bits (256 digital numbers)	16 bits (65,536 digital numbers)
Temporal resolution	16 days	16 days
Orbit characteristics	Sun-synchronous	Sun-synchronous
Inclination	98.2°	98.2°
Acquisition date	March 29 and October 7 (2001)	April 5 and October 14 (2021)
Sun Elevation	51.35°& 46.30°	56.89°& 46.36°
Cloud cover	0.0%, 0.0%	0.0%, 0.0%
Map projection and datum	UTM zone 36, World Geodetic System 84 (WGS 84)	UTM zone 36, WGS 84

Conversion of digital number values into top of atmosphere reflectance and data correction for the sun elevation effect

In order to compute accurate vegetation indexes, it is better not to use pixel radiance values; instead, it is better to use ToA-corrected R and NIR bands for calculating indexes than surface-corrected reflectance, which is a more complex issue. Surface reflectance (SR) estimation is the most critical preprocessing step for deriving geophysical parameters in multi-sensor remote sensing (Bilal *et al*., 2019). As a time-series analysis is adopted in this study, it is fundamental and necessary to interpret spectral images in terms of physically meaningful and quantifiable value that depicts surface features, which is deficient with the DN values. The reflectance values from the satellite data of Landsat 5 TM and Landsat 8 OLI were calculated. Landsat 5 TM and Landsat 8 OLI spectral radiance data were also converted to planetary ToA reflectance using coefficients of reflectance rescaling available in their files (Table 2). For converting DN values into ToA, reflection in the TM and OLI images were substituted in the following equation:

$$\rho\lambda' = M\ \rho Qcal + A\ \rho \quad \text{…… equation 1}$$

where ρλ' is the ToA planetary reflectance, without correction for the solar angle, M ρ is the band-specific multiplicative rescaling factor from the metadata, A ρ is the band-specific additive rescaling factor from the metadata, and Qcal is the quantized and calibrated standard product pixel values (DN).

In order to reduce the effect of the sun elevation, the reflectance value of the four images with the sun angle were corrected using the following equation:

$$\rho\lambda = \rho\lambda\ '/\sin\theta SE \quad \text{…… equation 2}$$

where ρλ is the ToA planetary reflectance and θSE is the local sun elevation angle. The scene center sun elevation angle in degrees is provided in the metadata of the images (Sun Elevation)

Table (2): Coefficients of reflectance rescaling for Landsat 5 TM and Landsat 8 OLI.

	Red band (R)		**Near infrared band (NIR)**	
	additive rescaling factor	multiplicative rescaling factor	additive rescaling factor	multiplicative rescaling factor
Landsat 5 TM	-0.004662	0.0021985	-0.007248	0.0026610
Landsat 8 OLI	-0.100000	0.00002	-0.100000	0.00002

At this stage in the study, the four preprocessed satellite data images were ready for the calculation of the NDVI between NIR and R (images for 2001 and 2021; equation 3):

NDVI = (NIR − R)/(NIR + R) …… equation 3

In Landsat 5 TM, band 3 is the R band, and band 4 is the NIR band, while in Landsat 8 OLI, band 4 is the R band, and band 5 is the NIR band. The degree of greenness is equivalent to the chlorophyll concentration. NDVI values vary with the absorption of red light by plant chlorophyll and the reflection of infrared radiation by water-filled leaf cells (Gandhi *et al*., 2015).

To evaluate the changes in NDVI, the resulting images were subtracted with positive NDVI and negative NDVI changes with a resolution of 30x30 m of the pixel (equations 4, 5, and 6):

ΔNDVI_2001 = NDVI October 7 − NDVI March 29……. equation 4

ΔNDVI_2021 = NDVI October 14 − NDVI April 5…… equation 5

ΔNDVI 2001_2021= ($NDVI_{2021}$ April 5 +October 14)/2 – ($NDVI_{2001}$ March 29 + October 7)/2 …… equation 6

To realize the effect of sun elevation correction on the four images, the NDVI was calculated before and after the preprocessing procedures of the satellite data, although emphasis in this study is laid on the atmospherically corrected data.

Results and Discussion

Conversion of DN values of the four image dates into the ToA reflectance and the correction of data for the sun elevation angle positively affected values of their NDVI, as shown in table 3. This is because the preprocessing step decreased the pixel values of the R band and increased those values for the NIR band.

Table (3): NDVI values of the four image dates before and after the correction for the sun elevation.

Image date	NDVI value before the correction for the sun elevation	NDVI value after the correction for the sun elevation
March 29, 2001	-0.4339 to 0.7950	-0.3776 to 0.8477
October 7, 2001	-0.6190 to 0.6800	-0.6137 to 0.7474
April 5, 2021	-0.2140 to 0.5870	-0.4767 to 0.8501
October 14, 2021	-0.2020 to 0.4860	-0.4335 to 0.8398

NDVI values area estimation for the four image dates

The NDVI of images were reclassified and colored, in order to get descriptive meaningful classes. As mentioned before, the NDVI values range between -1 and +1. The stretched values of the NDVI for each image were reclassified into five land cover classes using the manual classification method. Each class was given a descriptive meaning in terms of vegetation cover (Table 4).

Table (4): Reference values used for the reclassification of the NDVI values for the four image dates.

	NDVI value	Description of class
1	-1.000 to 0.000	Water and clouds
2	0.000 to 0.100	Bare soil and rocks
3	0.100 to 0.200	Sparse green vegetation cover
4	0.200 to 0.600	Moderate-to-dense green vegetation cover
5	>0.600	Dense green vegetation cover

NDVI area estimation for the image acquired on March 29, 2001

This image represents the vegetation cover status in the spring 2001 from Landsat 5 TM. The count of pixels for each class was converted to an area in km² using the following expression:

class area (km²) = count*30m*30m/1000000m.

Table (5): Area estimation of NDVI classes for the corrected image acquired on March 29, 2001

	NDVI class value	Description	Count of pixels	Area (km²)
1	-0.377 to 0.000	Water and moist soil	1,373	1.2356
2	0.000 to 0.100	Bare soil and rocks	811,775	730.5973
3	0.100 to 0.2000	Sparse green vegetation cover	1,458,522	1312.6700
4	0.200 to 0.600	Moderate-to-dense vegetation cover	3,921,682	3529.5140
5	0.600 to 0.848	Dense vegetation cover	79,659	71.6930
Total			**6,273,011**	**5645.7099**

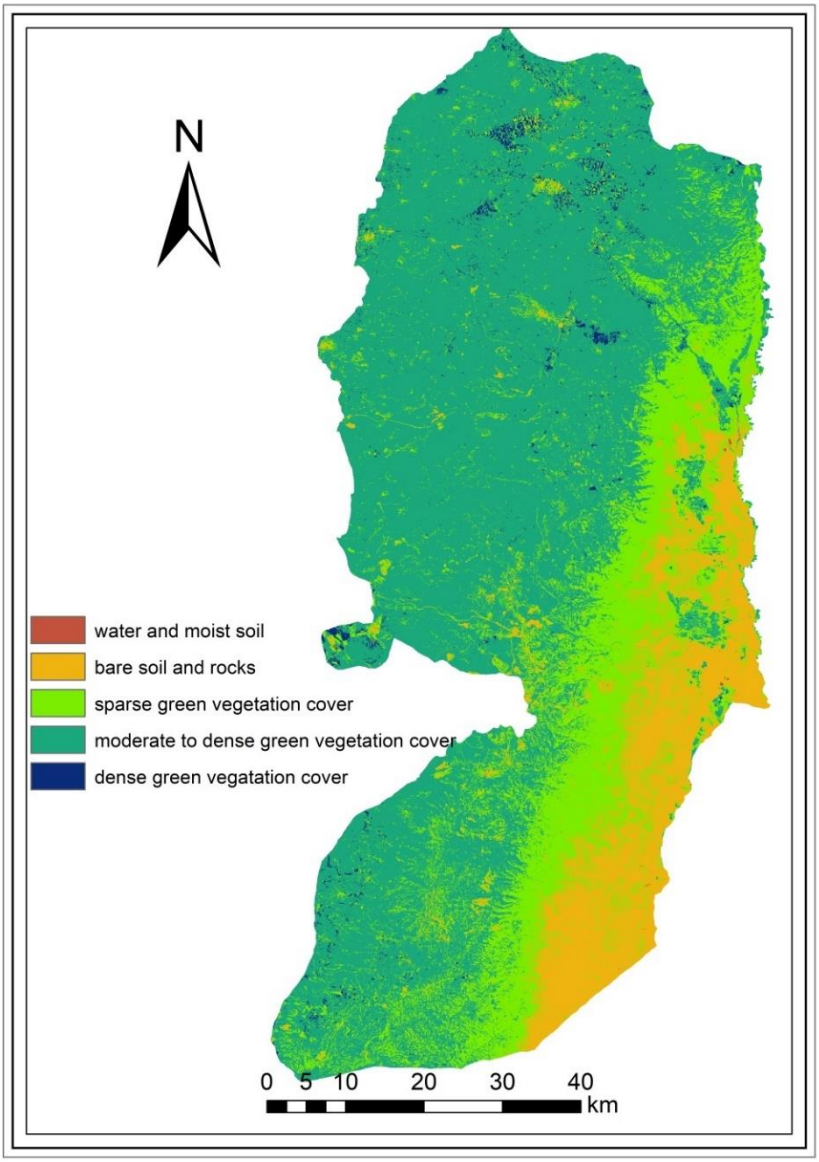

Figure (3): NDVI map of the West Bank derived from Landsat 5 TM image acquired on March 29, 2001

NDVI area estimation for the image acquired on October 7, 2001

This image represents the vegetation cover status in the autumn of 2001 from Landsat 5 TM. The count of pixels for each class was converted to area in km² using the same expression mentioned above.

Table (6): Area estimation of NDVI classes for the corrected image acquired on October 7, 2001

	NDVI class value	**Description**	**Count of pixels**	**Area (km²)**
1	-0.613 to 0.000	Water and moist soil	4,146	3.7314
2	0.000 to 0.100	Bare soil and rocks	3,318,096	2986.2861
3	0.100 to 0.200	Sparse green vegetation cover	268,3123	2414.8110
4	0.200 to 0.600	Moderate-to-dense vegetation cover	267,275	240.5475
5	0.600 to 0.747	Dense vegetation cover	371	0.3339
Total			**6,273,011**	**5645.7099**

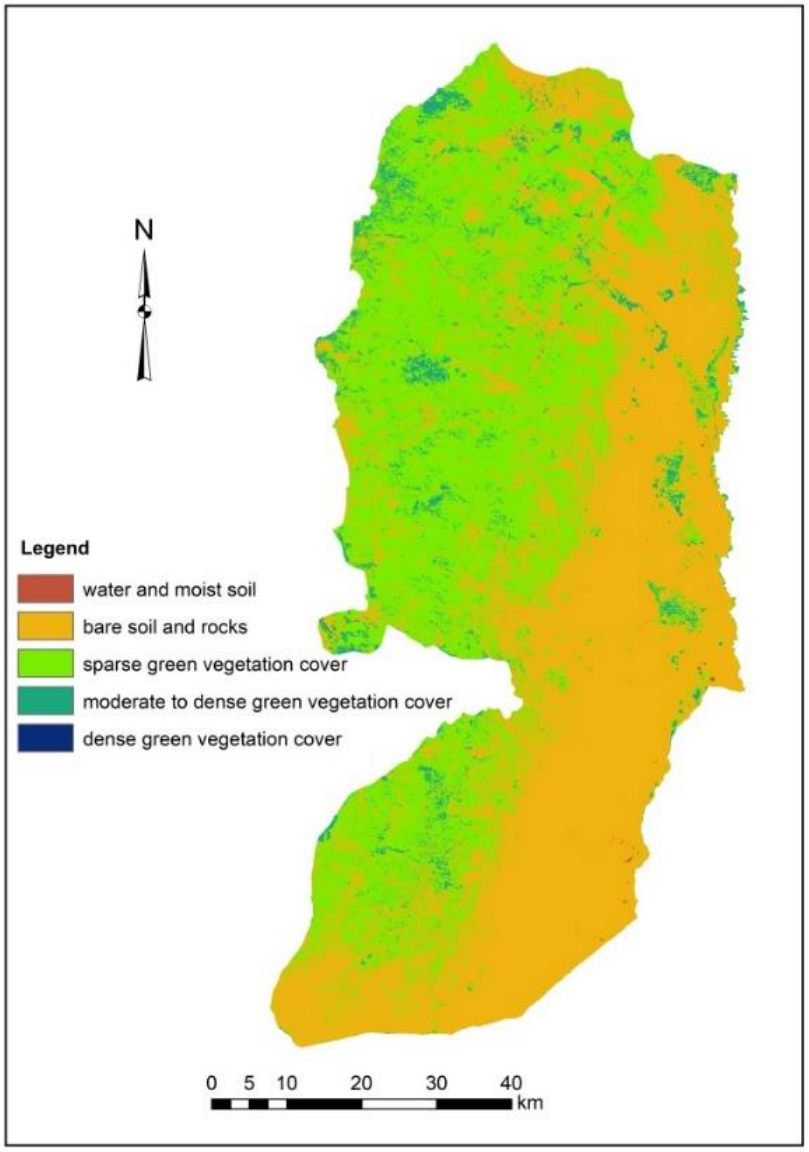

Figure (4): NDVI map of the West Bank derived from Landsat 5 TM image acquired on October 7, 2001

Table (7): NDVI class area change between spring and autumn 2001

	Description	Spring 2001 area (km²)	Autumn 2001 area (km²)	Autumn area − spring area (change/km²)
1	Water and moist soil	1.2356	3.7314	2.4957
2	Bare soil and rocks	730.5973	2986.2861	2255.6885
3	Sparse green vegetation cover	1312.6700	2414.8110	1102.141
4	Moderate-to-dense vegetation cover	3529.5140	240.5475	-3288.9665
5	Dense vegetation cover	71.6930	0.3339	-71.3592
Total		**5645.7099**	**5645.7099**	**0.00**

Table 7 and figures 3 and 4 depict big changes in the amount of NDVI areas on the one hand and its spatial distribution on the other hand. Bare soil and rocks class and the sparse green vegetation class increased considerably in autumn (2255.68 km² and 1102.14 km², respectively), while moderate and dense green vegetation decreased markedly (-3288.97 km² and -71.36 km², respectively).

The NDVI map of spring 2001 was subtracted from that of autumn 2001 using the raster calculation function in ArcGIS 10.8 software. Results presented in Table 8 show that the NDVI of 5582.297 km² or 98.89% of the surface area of the West Bank decreased in autumn by -0.81– 0 (negative change), while the NDVI of 63.4131 km² or 1.11% increased by 0– 0.67 (positive change).

Table (8): Spring − Autumn 2001 NDVI positive and negative change.

Description of change	Count of pixels	Changed area (km²)	% change
Negative	6,202,552	5582.2968	98.89
Positive	70,459	63.4131	1.11
	6,273,011	**5645.7099**	**100**

Figure 5 shows the spatial distribution of the NDVI seasonal change between spring and autumn 2001. The map shows that only limited areas in the Jordan Valley, the semi-coastal plains (Jenin plains, Tulkarem, and Qalqilia), and the intermediate plains of Hebron plateau have positive change. Those areas mostly represent irrigated crops. The rest areas of the West Bank have negative green vegetation change because all unmanaged green grass areas have dried and deciduous tree areas lost some of their leaves in autumn.

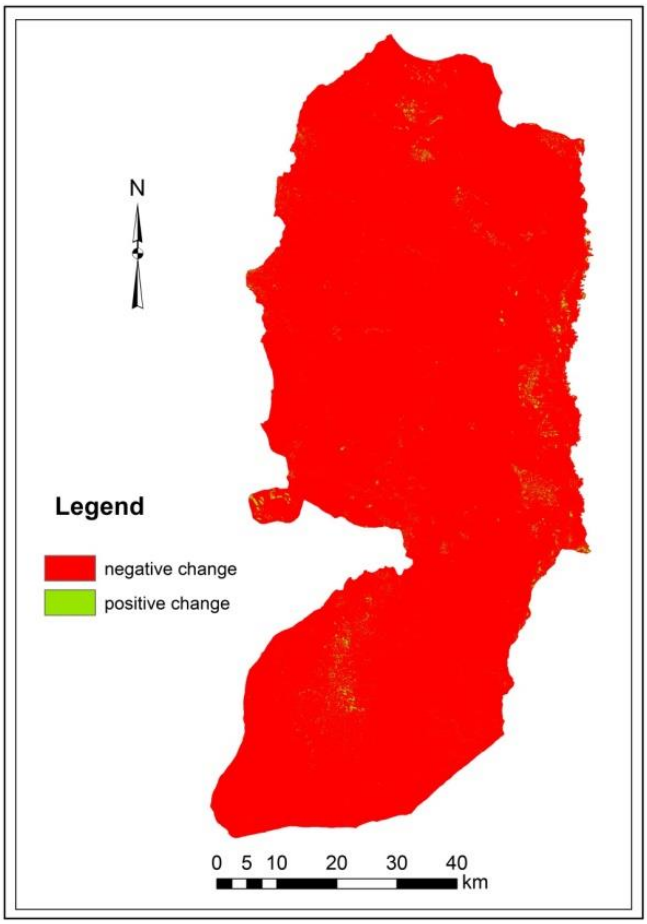

Figure (5): NDVI seasonal change between spring and autumn 2001

NDVI area estimation for the image acquired on April 5, 2021

This image represents vegetation cover status in spring 2021 from Landsat 8 OLI. The count of pixels for each class is converted to an area in km² (count*30*30/1000000).

Table (9): Area estimation of NDVI classes for the corrected image acquired on April 5, 2021

	NDVI class value	Description	Count of pixels	Area (km²)
1	-0.477–0.000	Water and moist soil	6,193	5.5735
2	0.000–0.100	Bare soil and rocks	127,486	114.7372
3	0.100–0.200	Sparse green vegetation cover	1,408,213	1267.3920
4	0.200–0.600	Moderate-to-dense vegetation cover	4,549,451	4094.5060
5	0.600–0.850	Dense vegetation cover	181,668	163.5012
Total			**6,273,011**	**5645.7099**

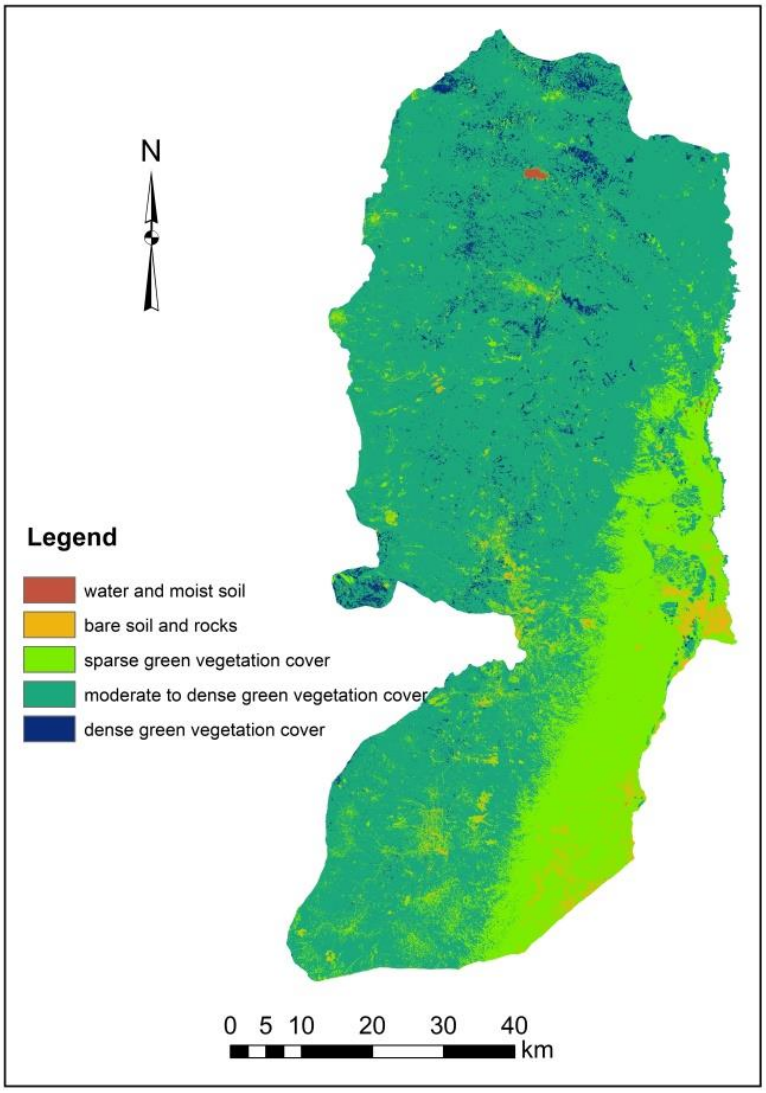

Figure (6): NDVI map of the West Bank derived from Landsat 8 OLI image acquired on April 5, 2021

Figure 6 shows that Marj Sanour in the mid-north of the West Bank contains some water, and its soil is moist. Also, the bare soil and rocks

cover class is mostly limited to the area of Jericho city. The sparse vegetation cover (mainly unmanaged grass) spread on the eastern slope region, and the moderate-to-dense green cover spread across most areas of the West Bank, whereas the dense green vegetation cover is limited to the plains of the northern West Bank. This high green cover distribution in spring 2021 is due to the relatively high amount of rainfall in 2020/2021 compared to that of spring 2001 (WAFA, 2022; PCBS, 2008).

NDVI area estimation for the image acquired on October 14, 2021

This image represents vegetation cover status in autumn 2021 from Landsat 8 OLI. The count of pixels for each class is converted to an area in km² as shown in Table 10.

Table (10): Area estimation of NDVI classes for the corrected image acquired on October 14, 2021

	NDVI class value	Description	Count of pixels	Area (km²)
1	-0.477 to 0.000	Water and moist soil	400	0.3600
2	0.000 to 0.100	Bare soil and rocks	28,066	25.2592
3	0.100 to 0.200	Sparse green vegetation cover	2,994,380	2694.9420
4	0.200 to 0.600	Moderate-to-dense vegetation cover	3,244,523	2920.0800
5	0.600 to 0.850	Dense vegetation cover	5,632	5.0687
Total			**6,273,011**	**5645.7099**

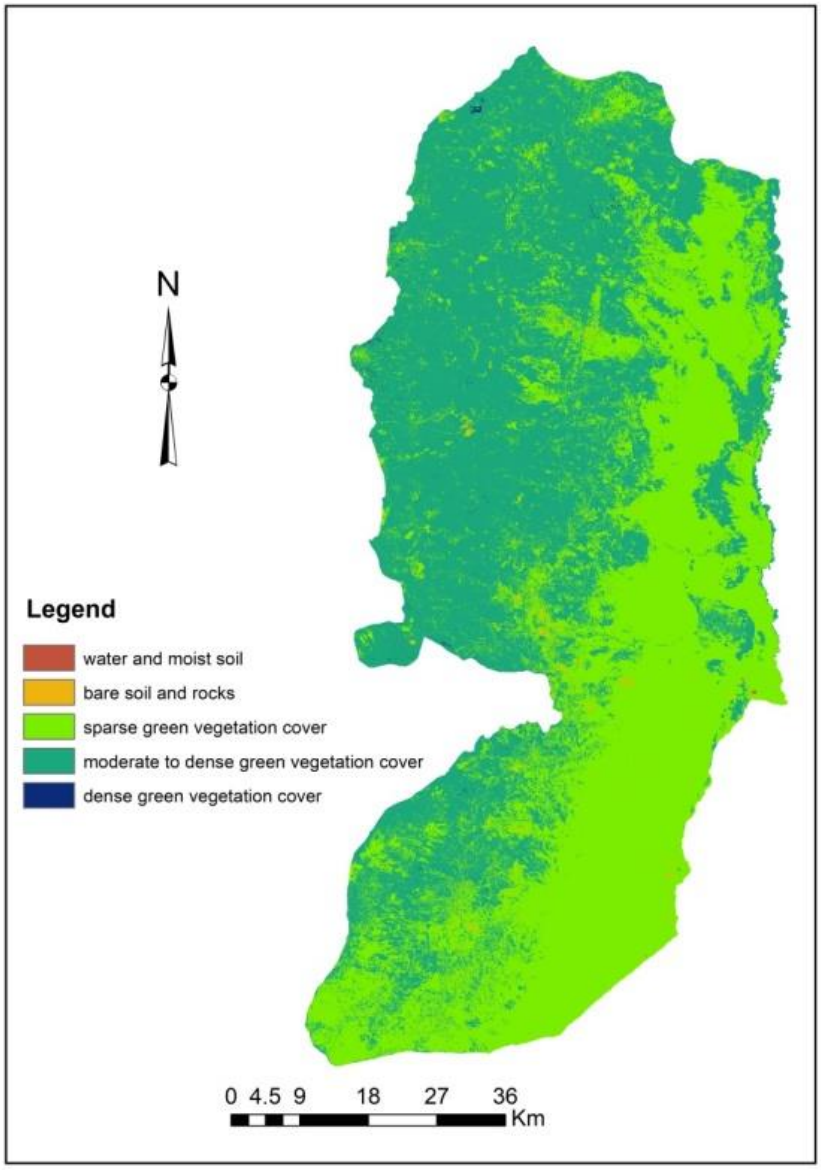

Figure (7): NDVI map of the West Bank derived from Landsat 8 OLI image acquired on October 14, 2021

Figure 7 shows that the sparse vegetation cover and the moderate-to-dense vegetation cover class represent the majority of the study area in autumn 2021. The dense vegetation cover and the moist soil classes represent small patches of land.

Table (11): NDVI class area change between spring and autumn 2021

	Description	**Spring 2021 area (km²)**	**Autumn 2021 area (km²)**	**Autumn area − spring area (change/km²)**
1	Water and moist soil	5.5735	0.3600	-5.2135
2	Bare soil and rocks	114.7372	25.2592	-89.4780
3	Sparse green vegetation cover	1267.3920	2694.9420	1427.5500
4	Moderate-to-dense vegetation cover	4094.5060	2920.0800	-1174.4260
5	Dense vegetation cover	163.5012	5.0687	-158.4325
Total		**5645.7099**	**5645.7099**	**0.00**

Table 11 and figures 6 and 7 illustrate big seasonal changes in the amount of the NDVI areas on the one hand, and its spatial distribution on the other hand. The sparse green vegetation class increased considerably in autumn (1427.55 km²), while moderate and dense green vegetation decreased to a great extent (-1174.426 km² and -158.4325 km², respectively).

The NDVI map of spring 2021 was subtracted from that of autumn 2021. Results presented in Table 12 show that the NDVI of 4561.201 km² or 80.79 percent of the surface area of the West Bank decreased in autumn by -0.71 to 0 (negative change), while the NDVI of 1084.509 km² or 19.21 percent is increased by 0– 0.97 (positive change).

Table (12): Spring − Autumn 2021 NDVI positive and negative change.

Description of change	Count of pixels	Changed area (km^2)	% change
Negative	5,068,001	4561.201	80.79
Positive	1,205,010	1084.509	19.21
	6,273,011	**5645.7099**	**100**

Figure 8 shows the spatial distribution of the NDVI seasonal change between spring and autumn 2021. The map shows that areas in the Jordan Valley and the eastern slopes (19.21 percent) of the West Bank have positive change. Those areas mostly represent irrigated crops, and their soil is dry in autumn. The rest area of the West Bank has negative green vegetation change, because all unmanaged green grass areas have dried and deciduous tree areas lost some of their leaves in autumn.

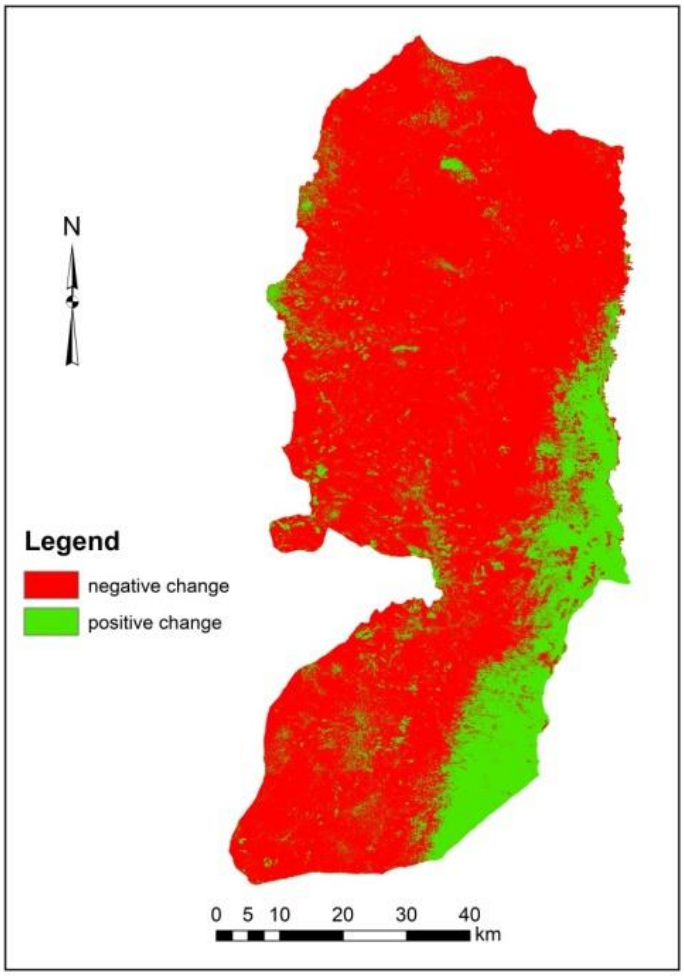

Figure (8): NDVI seasonal change between spring and autumn 2021

Statistical characteristics of the NDVI for the four image dates

To understand the status of the NDVI of the study area from the four satellite images, the main statistics, i.e., their minimum, maximum, mean, and standard deviation were calculated using ArcGIS 10.8 software. Table 13 shows the statistical characteristics of the West Bank NDVI.

Table (13): Statistical characteristics of the West Bank NDVI.

	Date of image	Minimum	Maximum	Mean	Standard deviation
1	March 29, 2001	-0.38	0.85	0.25	0.13
2	October 7, 2001	-0.61	0.75	0.11	0.05
3	April 5, 2021	-0.48	0.85	0.32	0.15
4	October 14, 2021	-0.43	0.84	0.22	0.08

Table 13 shows that the mean NDVI of 2021 in both seasons under consideration is much better than that of 2001. Also, the table shows that the greenness of autumn 2001 is relatively low compared to that of 2021 (0.11 and 0.22, respectively).

NDVI change between 2001–2021

Equation 6 was used to calculate changes in NDVI between 2001 and 2021. The raster calculator was used to subtract the average NDVI of 2001 from that of 2021, then the resultant raster map was reclassified in ArcGIS 10.8, producing a new map representing the NDVI change. The NDVI change map was reclassified into two classes: one representing a negative change and the other representing a positive change (Figure 9). Counts of pixel change were converted into a change in km² (Table 14).

Table (14): Area estimation of NDVI change between 2001 and 2021

Description of change	Count of pixels	Changed area (km²)	% change
Negative	570,451	513.4059	9.09
Positive	5,702,560	5132.3040	90.91
	6,273,011	**5645.7099**	**100**

Table 14 shows that a remarkable positive change of the NDVI occurred between 2001 and 2021. This positive change is ascribable to the higher annual rainfall in 2021 than that of 2001 over most regions of the West Bank, and the conversion of areas in the West Bank from rain-fed agriculture to irrigated agriculture system. Figure 9 shows that the negative

change areas are concentrated in and around the urban area, mainly the main cities. This indicates that the urban built-up areas have extended to the neighboring agricultural lands (Ghodieh, 2019).

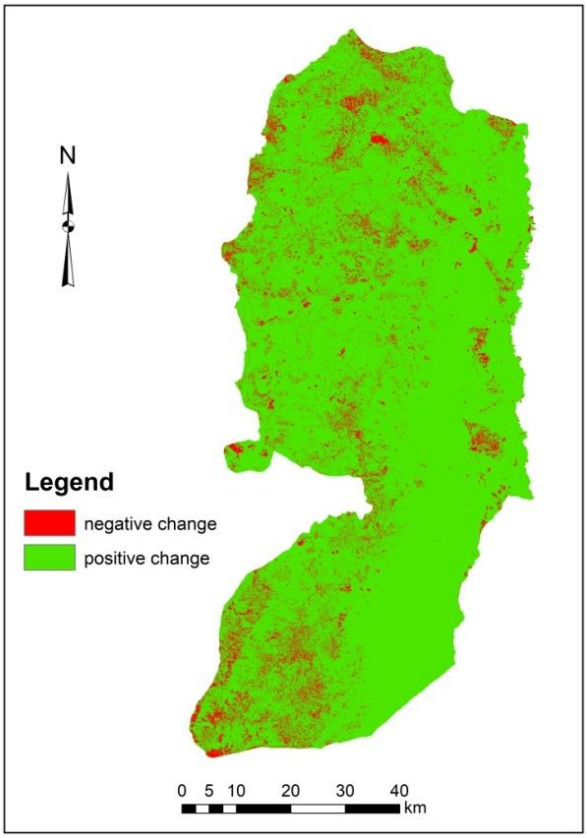

Figure (9): NDVI change between 2001 and 2021

Conclusion

Results of the study showed that the moderate resolution of satellite images (30*30m) is suitable for studying the NDVI change in the West Bank. Results also showed that the NDVI values of both image dates (2001 and 2021) have considerable seasonal change between spring and autumn. The negative change of the NDVI of autumn for both dates is much higher

than the positive change. About 98.89% of the West Bank area scored a negative change in 2001, while about 80.79% of the West Bank scored a negative change in 2021. Positive NDVI change in 2001 is limited to small areas of the Jordan Valley and irrigated agriculture in the plains of the northern West Bank. Concerning the positive NDVI change in 2021, it is concentrated in the eastern slopes of the West Bank, in addition to the Jordan Valley. Results also showed that the higher rainfall amount in 2021 improved the NDVI of this year.

Results further revealed a considerable positive change in the NDVI between 2001 and 2021. Around 90.91 percent of the surface area of the West Bank (5132.304 km²) has positive change, while only 9.09 percent has negative change. This is mainly attributable to the relatively high rainfall amount of 2021, and the conversion from rain-fed agriculture to an irrigated agricultural system, mainly in the northern West Bank plains. The negative change areas are concentrated in and around the urban built-up areas, and this indicates that the urban expansion is at the expense of agricultural lands.

The positive change in green vegetation cover in 2021 is temporary because it represents the grasses and weeds that are green in spring and dry in summer. So, it is recommended that decision-makers and policymakers in the Ministry of Agriculture and environmental organizations prepare plans to increase permanent green spaces in the West Bank, mainly in the arid and semi-arid regions. Furthermore, increasing green spaces contributes to facing climate change and global warming.

References

– Abuelaish, B. & Olmedo, M. T. C. (2016). Scenario of land use and land cover change in the Gaza Strip using remote sensing and GIS models. *Arabian Journal of Geosciences*, *9*(4), 1-14.

– Applied Research Institute of Jerusalem. (2003). Climatic zoning for energy efficient buildings in the Palestinian territories (the West Bank and Gaza). *ARIJ*, Jerusalem.

- Bilal, M. Nazeer, M. Nichol, J. E. Bleiweiss, M. P. Qiu, Z. Jäkel, E. ... & Lolli, S. (2019). A simplified and robust surface reflectance estimation method (SREM) for use over diverse land surfaces using multi-sensor data. *Remote Sensing*, *11*(11), 1344.
- Buchhorn, M. Raynolds, M. K. & Walker, D. A. (2016). Influence of BRDF on NDVI and biomass estimations of Alaska Arctic tundra. *Environmental Research Letters*. *11*(12). 125002.
- Chen, W. Blain, D. Keohler, J. & Fraser, R. (2009). Biomass measurements and relationships with Landsat-7/ETM+ and JERS-1/SAR data over Canada's western sub-arctic and low arctic. *Int. J. Remote Sens*. 30 2355–2376.
- FRIEDL, M. Hodges, J. & Zhang, XY. (2002). Global land cover mapping from MODIS: Algorithms and early results. *Remote Sensing of Environment*, 83, pp. 287–302.
- Gandhi, M. Parthiban, S. Thummalu, N. & Christy, A. (2015). Ndvi: Vegetation change detection using remote sensing and gis – A case study of Vellore District. *Procedia Computer Science* 57, 1199 – 1210.
- Ghodieh, A. (2019). Urban Built-Up Area Estimation and Change Detection of the Occupied West Bank, Palestine, Using Multi-temporal Aerial Photographs and Satellite Images. *Journal of the Indian Society of Remote Sensing* https://doi.org/10.1007/s12524-019-01073-8.
- Gutman, G. (1999). On the use of long-term global data of land reflectances and vegetation indices derived from the advanced very high-resolution radiometer. *journal of geophysical research*, vol. 104, no. d6, pages 6241-6255.
- Hamada, S. & Ghodieh, A. (2021). Mapping of Solar Energy Potential in the West Bank, Palestine Using Geographic Information Systems. Papers in Applied Geography, 7:3, 256-273, DOI: 10.1080/23754931.2020.1870540.1951

- Huang, S. Tang, L. Hupy, J. P. Wang, Y. & Shao, G. (2021). A commentary review on the use of normalized difference vegetation index (NDVI) in the era of popular remote sensing. *Journal of Forestry Research*, *32*(1), 1-6.
- Huang, W. Huang, J. Wang, X. Wang, F. & Shi, J. (2013). Comparability of red/near-infrared reflectance and NDVI based on the spectral response function between MODIS and 30 other satellite sensors using rice canopy spectra. *Sensors*, *13*(12). 16023-16050.
- Jin, X., Wan, L., Zhang, Y. K., Hu, G., Schaepman, M. E., Clevers, J. G. P. W., & Su, Z. B. (2009). Quantification of spatial distribution of vegetation in the Qilian Mountain area with MODIS NDVI. *International Journal of Remote Sensing*, *30*(21), 5751-5766.
- Ju, Y. & Bohrer, G. (2022). Classification of Wetland Vegetation Based on NDVI Time Series from the HLS Dataset. *Remote Sensing*, *14*(9), 2107.
- Ma, X. Huete, A. Tran, N. N. Bi, J. Gao, S. & Zeng, Y. (2020). Sun-angle effects on remote-sensing phenology observed and modelled using himawari-8. *Remote Sensing*, *12*(8). 1339.
- Matese, A. & DiGennaro, S. (2021). Beyond the traditional NDVI index as a key factor to mainstream the use of UAV in precision viticulture. *Scientifc Reports, natureportfolio* |11:2721| https://doi.org/10.1038/s41598-021-81652-3.
- Mokarram, M. & Sathyamoorthy, D. (2015). Modeling the relationship between elevation, aspect and spatial distribution of vegetation in the Darab Mountain, Iran using remote sensing data, Model. *Earth Syst. Environ*. 1:30 DOI 10.1007/s40808-015-0038-x.
- Mokarram, M. Soleimanpour, L. & Hojati, M. (2016). Applied remote sensing for determination of vegetation Index. *Journal of Environment* (2016), Vol. 5, Issue 2, pp. 19-23.

- Naif, S. S. Mahmood, D. A. & Al-Jiboori, M. H. (2020). Seasonal normalized difference vegetation index responses to air temperature and precipitation in Baghdad. *Open Agriculture*, *5*(1), 631-637.
- Robinson, N. P. Allred, B. W. Jones, M. O. Moreno, A. Kimball, J. S. Naugle, D. E. ... & Richardson, A. D. (2017). A dynamic Landsat derived normalized difference vegetation index (NDVI) product for the conterminous United States. *Remote sensing*, *9*(8), 863.
- Ndungu, L. Oware, M. Omondi, S. Wahome, A. Mugo, R. & Adams, E. (2019). Application of MODIS NDVI for Monitoring Kenyan Rangelands Through a Web Based Decision Support Tool. Front. *Environ. Sci*. 7:187. doi: 10.3389/fenvs.2019.00187.
- Palestinian Central Bureau of Statistics (PCBS). (2008). Meteorological Conditions in the Palestinian Territory, Annual Report.
- Palestinian News and Info Agency_WAFA (2022). https://info.wafa.ps/ar_page.aspx?id=2226
- Pettinari, M. Chuvieco, E. Padilla, M. Storm, Th. (2016). ESA CCI ECV Fire Disturbance: D1.4 Data Access Requirement Document, version 2.3. Available from: http://www.esa-fire-cci.org/documents
- Singh, P. & Javeed, O. (2021). NDVI Based assessment of land cover changes using remote sensing and GIS-(A case study of Srinagar district, Kashmir). *Sustainability, Agri, Food and Environmental Research*, (ISSN: 0719-3726), 9(4), 2021: 491-504 http://dx.doi.org/10.7770/safer-V0N0-art2174
- Themistocleous, K. & Hadjimitsis, D. (2013). Development of an image based integrated method for determining and mapping aerosol optical thickness (AOT) over urban areas using the darkest pixel atmospheric correction method, RT equation and GIS: A case study of the Limassol area in Cyprus. *ISPRS Journal of Photogrammetry and Remote Sensing* 86, 1–10. http://dx.doi.org/10.1016/j.isprsjprs.2013.08.011.

- Towers, P.C. PobleteEcheverría, C. (2021). Effect of the Illumination Angle on NDVI Data Composed of Mixed Surface Values Obtained over Vertical-ShootPositioned Vineyards. *Remote Sens*., 13, 855. https://doi.org/ 10.3390/rs13050855.
- Weijiao, H. (2013). Comparability of Red/Near-Infrared Reflectance and NDVI Based on the Spectral Response Function between MODIS and 30 Other Satellite Sensors Using Rice Canopy Spectra. *Sensors*, 13, 16023-16050; doi:10.3390/s131216023.
- Zhai, Y. Roy, D. P. Martins, V. S. Zhang, H. K. Yan, L. & Li, Z. (2022). Conterminous United States Landsat-8 top of atmosphere and surface reflectance tasseled cap transformation coefficients. *Remote Sensing of Environment*, *274*, 112992.
- Yengoh, G. T. Dent, D. Olsson, L. Tengberg, A. E. & Tucker III, C. J. (2015). Use of the Normalized Difference Vegetation Index (NDVI) to assess Land degradation at multiple scales: current status, future trends, and practical considerations. *Springer*.
- Zaitunah, A. Ahmad, A. G. & Safitri, R. A. (2018, March). Normalized difference vegetation index (ndvi) analysis for land cover types using landsat 8 oli in besitang watershed, Indonesia. In *IOP Conference Series: Earth and Environmental Science* (Vol. 126, No. 1, p. 012112). IOP Publishing.
- Zhu, M. Zhang, J. & Zhu, L. (2021). Article Title Variations in Growing Season NDVI and Its Sensitivity to Climate Change Responses to Green Development in Mountainous Areas. Front. *Environ. Sci*. 9:678450. doi: 10.3389/fenvs.2021.678450.

